Investigation on Properties of New Fluorine- and Silicon-Modified UV-Cured Epoxy Methacrylate Resin

Chunyi Tang,[1,2] Weiqu Liu[1]

[1]*Guangzhou Institute of Chemistry, Chinese Academy of Sciences, Guangzhou 510650, People's Republic of China*
[2]*Graduate School of Chinese Academy of Sciences, Beijing 100049, People's Republic of China*

Received 21 July 2009; accepted 24 January 2010
DOI 10.1002/app.32164
Published online 29 March 2010 in Wiley InterScience (www.interscience.wiley.com).

ABSTRACT: Photosensitive organofluorine and organosilicon play a key role in improving the properties of UV-curing coating materials. In this study, by using 2,2,3,4,4,4-hexafluorobutyl methacrylate (HFMA) and a synthesized side methacryloxy group polysiloxane (MAPS) as modifying materials and bisphenol-A epoxy methacrylate (BEMA) as matrix, respectively, a innovative UV-curing system, BEMA/HFMA/MAPS composite system was developed. Through UV-cure process, a series of BEMA/HFMA, BEMA/MAPS, and BEMA/HFMA/MAPS cured composite films with different proportions were successfully obtained. It was found that HFMA monomer was helpful for the reduction of the surface energy of the UV-cured composite films and the enhancement of their water resistance property. Without HFMA in BEMA matrix, MAPS could facilitate the improvement of the properties of BEMA/MAPS cured films, and the presence of MAPS in BEMA/HFMA/MAPS system could significantly decrease the surface energy of the cured films to 22.1 mJ/m^2 and improve their thermal stabilities and water resistance properties by measurements, contact angle, TGA, DSC, and water resistance. To the SEM observation, HFMA and MAPS were well distributed in the cured films in favor of their excellent performances. © 2010 Wiley Periodicals, Inc. J Appl Polym Sci 117: 1859–1866, 2010

Key words: side methacryloxy group polysiloxane; 2,2,3,4,4,4-hexafluorobutyl methacrylate; bisphenol-A epoxy methacrylate; UV-cure; composite film

INTRODUCTION

Epoxy resins, characterized by the possession of more than one 1,2-epoxy groups per molecules as the active centers of the resins, are popular materials in coating industry. Since 1940s, because cured epoxy resins exhibit excellent adhesion, high strength, excellent electrical insulation, environmental stability, and good processability, their commercial introduction has widened the applications of synthetic products in various fields.[1-3] Then, when the epoxy resins with terminal unsaturated double bonds were generated, they were immediately used in UV-curing fields, like inks, optical fiber coatings, and electronic devices.[4-8] Among many kinds of UV-curable polymers, bisphenol-A epoxy methacrylate/acrylate resins are especially important. However, such resins have less photosensitive crosslinkable groups commonly. Moreover, thermal, surface and water resistance properties of their cured products are very sensitive to the chemical structure and component of the resins, crosslinking agent, the type and concentration of cure initiators, crosslinking reaction conditions in the radiation chamber. In point of these issues, researchers tried to use small molecular crosslink agent[9] or the form of interpenetrating polymer network,[10] but these methods could not improve the thermal, surface and water resistance properties simultaneously of the resins. Other study indicated hybrid nanocomposite UV-cured coatings were prepared by combining bisphenol-A ethoxylate (15 EO/phenol) dimethacrylate with methacrylic oligomer and multifunctional methacrylic polyhedral oligomeric silsesquioxane blocks (POSS), respectively.[11] Though the random structure obtained by the condensation of the methacrylic silica precursor showed a stronger effect on glass transition temperature (T_g) than that by the introduction of POSS, the postbaking treatment to samples caused the complicated technical process; and the water resistance would probably have no preferable variation. Hence, to improve thermal, water resistance, and surface properties of UV-curable epoxy resins needs to develop effective UV-curing system.

At present, the utilizations of organofluorine and organosilicon have received close attention, attributing to their unique characteristics including hydrophobicity, chemical stability, weathering resistance,

Correspondence to: W. Liu (liuwq@gic.ac.cn).
Contract grant sponsor: Scientific and Technological-Type, Small and Medium-Sized Enterprises Technology Innovation Fund Project of China Science and Technology Ministry; contract grant number: 06C26214401627.

good release properties, low coefficients of friction, water impermeability, and low refractive indices. To add these materials into epoxy resins can modify their properties to a great degree.[12] In fact, compared with the lower cost sources and more compatibility of organosilicon matrixes for multifunctional materials, although organofluorine can provide lower surface energy for materials, its high-cost source and the complicated synthesis process of fluorine-containing photosensitive polymers limited its broad uses in UV-curing industry.[13,14] Additionally, among organosilicon materials, UV-curable polysiloxanes have been produced and investigated. For example, ladder-like polysiloxane could be employed to cure with polyacrylate and improve scratch and abrasion resistance, higher gas barriers and temperature resistance;[15] and polydimethylsiloxane epoxy acrylate with terminal photosensitive groups was prepared and suitable for UV-curing optical fiber, metal and glass coating and solder mask materials for printed circuit.[16] Since polysiloxane provides two sites for cross-links and forms functional chains through bond formation with silicon it becomes a promising material for UV-curing areas.[17] Therefore, it is possible that the mixture of easy-to-get organofluorine monomer and polysiloxane with quantitative photosensitive groups can well facilitate surface, thermal and water resistance properties of epoxy resins.

Regarding this issue, in our work, firstly quantitative HFMA monomers were mixed with bisphenol-A epoxy methacrylate (BEMA) to form UV-cured composite films and the decreased degree of the surface energy of the cured films was investigated. Then methacryloxy group polysiloxane (MAPS) with a great number of photosensitive groups could be synthesized by the derivative reaction of a kind of polysiloxane and incorporated into BEMA matrix and HFMA/BEMA system, respectively. The surface energies of the cured films containing MAPS were further reduced, and MAPS increase the cross-link sites of systems so that their thermal and water resistance properties were enhanced simultaneously. By analyzes of contact angle, TGA, DSC and water resistance, the properties of the cured composite films were evaluated in detail, finally through SEM the internal morphologies were observed. As a result, we built up new UV-curing BEMA/HFMA/MAPS composite system.

EXPERIMENTAL

Materials

Allyl glycidyl ether (AGE) and polymethylhydrosiloxane (PMHS, 1.41 mol reactive proton per 100 g PMHS) were purchased from Xinghuo Chemical of China. Diglycidyl ether of bisphenol-A [DGEBA, Ep828, the epoxide equivalent weights (EEW): 196 g/epoxide] was from Shell Chemical in Shanghai city of China. Hydrogen hexachloroplatinate hydrate (Pt-catalyst), tetrabutylammonium bromide, and benzophenone were from Aldrich Chemical of USA. Ethylene glycol, methacrylic acid (MA), triethanolamine, and 2,2,3,4,4,4-hexafluorobutyl methacrylate (HFMA) were obtained from Tianjing Kemiou Chemical of China. All solvents were reagent grade or were purified by standard methods.

Synthesis of side methacryloyloxy group polysiloxane

The synthesis of MAPS was a two-step reaction. 21 g PMHS, 50 g toluene and an excess of AGE (1.5 equivalents of Si—H) were first charged into a 250 mL four-necked flask with stirrer, thermometer, and reflux condenser. When the solution was heated to 75°C, 1 wt % of Pt-catalyst was added to the flask under nitrogen and stirred until the end of reaction (the disappearance of absorption peak of the Si—H). Side epoxy polysiloxane (SEPS) was obtained by removing the excess AGE and the solvent using the rotary evaporator. Subsequently, to a four-necked flask with 20.1 g of SEPS and 50 mL toluene, 9.3 g MA (mole ratio of carboxyl to epoxy was 1 : 1) containing 0.12 g tetrabutylammonium bromide was added dropwise at 80°C for 30 min under stirring. The reaction was then carried out at 95°C to reach 98.9% of the conversion determined by the acid value. After toluene and unreacted MA were discarded by reduced pressure distillation, the product was obtained and labeled as MAPS.

Synthesis of bisphenol-A epoxy methacrylate resin

DGBEMA (80.3 g) was added to a four-necked flask and stirred at 85°C. A mixture of 35.3 g MA and 0.48 g tetrabutylammonium bromide was then added dropwise. The synthesis was proceeded at 100°C for 6 h to obtain BEMA with desired acid value (98.5% of the conversion). The disappearance of the absorption peak of epoxide group (910 cm^{-1}) and the appearance of the characteristic absorption peaks of C=C (1635 cm^{-1}) and C=O (1732 cm^{-1}) in FTIR spectra marked the completion of the reaction basically.

UV-cure

The UV-curing formulations were prepared by adding different contents of HFMA, MAPS, or both HFMA and MAPS to BEMA. The relative weight compositions for the different mixture are listed in Table I, and the chemical structures of these components are shown in Figure 1. The obtained mixtures were added of 5 wt % of 2 : 3 (w/w) benzophenone/

TABLE I
Weight Composition of UV-Curing Formulations

Sample	BEMA (g)	HFMA (g)	MAPS (g)
BEMA	100	–	–
BEMA/HFMA-1	100	5	–
BEMA/HFMA-2	100	10	–
BEMA/HFMA-3	100	15	–
BEMA/HFMA-4	100	20	–
BEMA/MAPS-1	100	–	5
BEMA/MAPS-2	100	–	10
BEMA/MAPS-3	100	–	15
BEMA/MAPS-4	100	–	20
BEMA/HFMA/MAPS-1	100	10	5
BEMA/HFMA/MAPS-2	100	10	10
BEMA/HFMA/MAPS-3	100	10	15
BEMA/HFMA/MAPS-4	100	10	20

triethanolamine as photoinitiator system. The UV-curable compounds were applied to glass, copper and wood plates, respectively (thickness of the final coating: 100 ± 10 μm) and irradiated for 20 s by a high-pressure mercury lamp (500 W) with a distance of 20 cm from lamp to the surface of samples in air atmosphere.

Characterization

FTIR was recorded with RFX-65A FRIR (Anatect, USA). ^{1}H-NMR was performed on a 400 MHz Brüker NMR spectrometer made in Switzerland using $CDCl_3$ as solvent and tetramethylsilane as the internal reference.

The contact angles of water and ethylene glycol were measured on the air-side surface of the coatings with a contact goniometer (Erma Contact Anglemeter, Model G-I, 13-100-0, Japan) by the sessile drop method with a microsyringe at 30°C. More than 10 readings were averaged to get a reliable value for each sample. In this study, the surface energy was calculated by using an indirect method, geometric-mean equation which was indicated by Owens and Wendt[18]: the surface energy of a given solid can be determined using the following equation applied to two liquids:

$$(1 + \cos\theta)\gamma_l = 2(\gamma_s^d \gamma_l^d)^{1/2} + 2(\gamma_s^{nd} \gamma_l^{nd})^{1/2} \quad (1)$$

where γ_s and γ_l are the surface free energies of the solid and pure liquid, respectively. The superscripts "d" and "nd" represent the dispersive and nondispersive contributions to total surface energy, respectively. According to Pinnau I, the contact angle, θ, in eq. (1) was obtained from the following equation[19]:

$$\theta = \cos^{-1}\left(\frac{\cos\theta_a + \cos\theta_r}{2}\right) \quad (2)$$

where θ_a and θ_r are the advancing and receding contact angles, respectively. To measure the contact angles of two liquids on a coating surface will gain two simultaneous equations for eq. (1) and readily solve γ_s^d and γ_s^{nd}. As a result, an estimated value of the total surface free energy, γ_s will be from the sum of the two components, γ_s^d and γ_s^{nd}, via assuming linear additives of the intermolecular forces (i.e., the dispersive and nondispersive forces). Water (γ_l = 72.8 mJ/m^2; γ_l^d = 21.8 mJ/m^2; γ_l^{nd} = 51 mJ/m^2) and ethylene glycol (γ_l = 48 mJ/m^2; γ_l^d = 29 mJ/m^2; γ_l^{nd} =19 mJ/m^2) were selected in this research.

The thermogravimetric analysis (TGA) was carried out by a Perkin–Elmer thermogravimetric analyzer made in USA at a heating rate of 10°C/min under nitrogen atmosphere in the temperature range of 50–600°C. The sample was about 6.5 mg. DSC measurement was performed on a TA Q200 differential scanning calorimeter made in USA, under nitrogen atmosphere. Specimen was heated from 0 to 150°C, at a heating rate of 20°C/min.

For the evaluation of water resistance, one method was that three kinds of plates, glass, copper, and wood coated with these UV-cured materials were immersed in distilled water for 5 days, and meanwhile their appearances were observed.

Another method was to measure water absorption ratio of the solid sample by putting the fresh film which was removed from the substrate carefully and

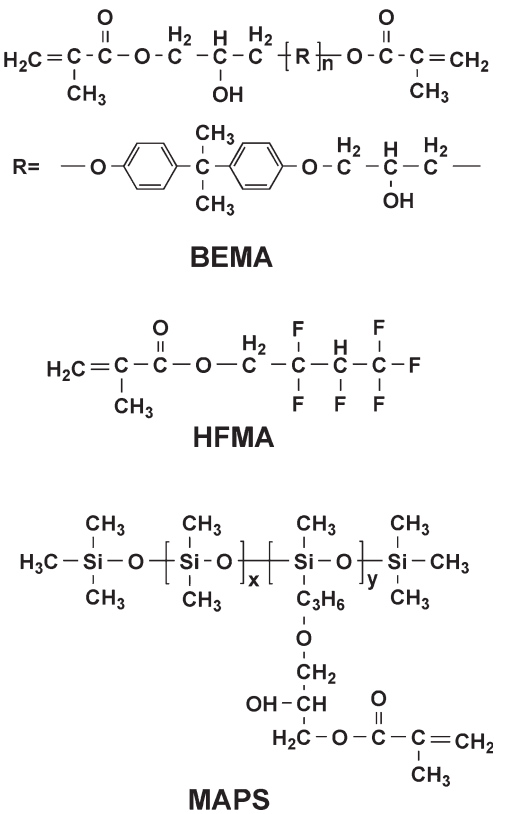

Figure 1 Chemical structures of the main UV-curable components.

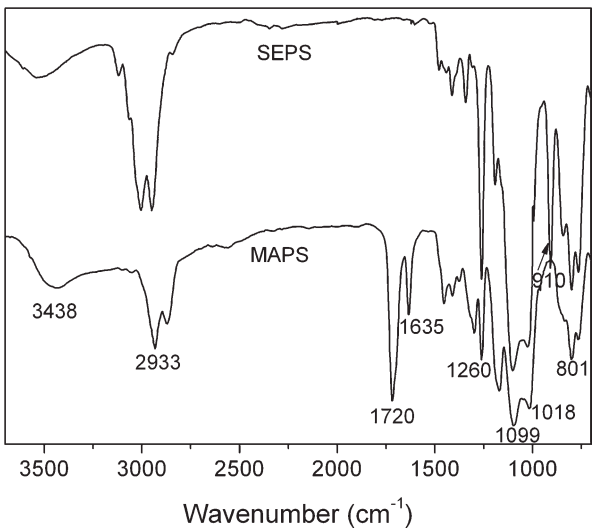

Figure 2 FTIR spectra of SEPS and MAPS.

dried for 24 h in vacuum under 60°C in advance, into boiling water for 24 h. Then the film was taken out and free water on the film surface was absorbed by filter paper. The saturated water absorption was calculated as follows:

$$\varpi = \frac{m_w - m_d}{m_d} \times (100\%)$$

where m_w and m_d are the mass of wet and dry film, respectively.

The cross section morphologies of the cured films were studied by scanning electron microscopy (Hitachi S-4300, Tokyo, Japan).

RESULTS AND DISCUSSION

Characterizations of the synthesized products

During the tow-step reaction process, PMHS was epoxidized, i.e., Si—H peak at 2156 cm^{-1} was disappeared basically, followed by the modification of MA which provided side methacryloxy group containing unsaturated double bonds (Fig. 2). In addition, the FTIR spectrum of MAPS exhibits that the two peaks at 1635 cm^{-1} and 1720 cm^{-1} are attributed to C=C and C=O stretching vibration, respectively, replacing the band of epoxide group at 910 cm^{-1} (Fig. 2). Meanwhile, the spectra present the characteristic absorption peaks at 801 and 1260 cm^{-1} for Si—CH_3, at 1018–1099 cm^{-1} for Si—O—Si, at 2933 cm^{-1} for C—H, and at 3438 cm^{-1} for —OH.

In the ^{1}H-NMR spectra of SEPS and MAPS (Fig. 3), peaks in the chemical shift range of 0.46–0.50, 1.54–1.60, 2.57, 2.77, 3.33, and 3.32–3.50 ppm were designated to methylenes and methines of the side groups, while peaks in 1.93, 5.56, and 5.64 ppm belonged to protons of methacryloyl group, indicating that epoxide groups were consumed in the reaction with methacrylic acid. Both of FTIR and ^{1}H-NMR spectra confirmed the chemical structure of the MAPS

Surface property of UV-cured composite films

It is well known that fluorine and silicone are low-surface tension materials. In this work, by the most natural approach of measuring the contact angle of a liquid drop on the film surface the relative wettability was determined, as summarized in Table II. For the measured contact angle values of BEMA/HFMA cured composite film surfaces, there is not obvious difference between them, while they are larger than that of BEMA cured film. As mentioned earlier, in view of relatively low-surface energy fluorine had a strong tendency to spread to surface.[20] Hence, when blended into the selected curing system, HFMA tended to move towards the film surface, and consequently imparted the surface hydrophobic function to some extent [Fig. 4(a)]. For the BEMA/MAPS cured film surfaces, in the presence of hydrophobic silicon, their contact angles are also lager than that of BEMA cured film. Moreover, because the silicon-oxygen chains could form cross-link network, BEMA/MAPS films showed more hydrophobic than BEMA/HFMA films [Fig. 4(b)]. In Table II, both advancing and receding contact angles increase upon the increasing MAPS content, i.e., the surfaces of BEMA/HFMA/MAPS cured composite films become much more hydrophobic than BEMA film, and the increased degree of the contact angles is much higher than that of sample BEMA/HFMA and BEMA/MAPS series. Such can be attributed to hydrophobic components, not only fluorine-

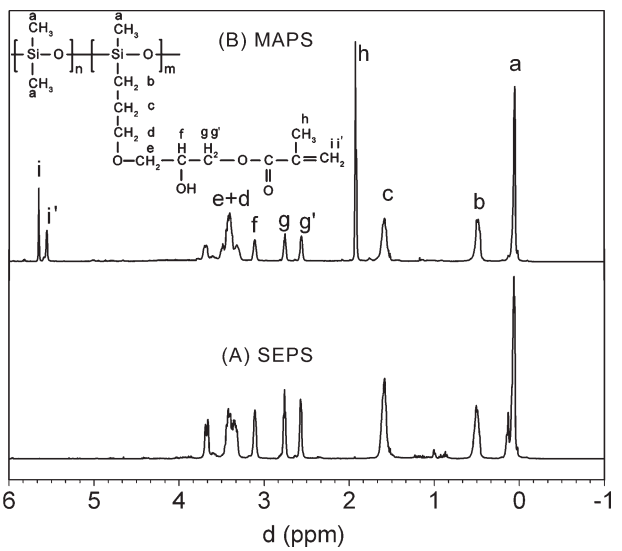

Figure 3 ^{1}H-NMR spectra of SEPS and MAPS.

TABLE II
Contact Angles and Surface Energies of The UV-Cured Composite Films

Sample	Water (°)		Ethylene glycol (°)		Surface energy (mJ/m^2)		
	θ_a	θ_r	θ_a	θ_r	γ_s^d	γ_s^{nd}	γ_s
BEMA	65.2 ± 2.1	55.1 ± 2.0	58.0 ± 2.0	48.4 ± 2.0	4.1 ± 0.5	40.1 ± 3.9	44.1 ± 3.4
BEMA/HFMA-1	74.2 ± 2.0	60.1 ± 2.1	55.4 ± 2.0	42.5 ± 2.0	12.1 ± 0.2	23.3 ± 3.5	35.3 ± 1.6
BEMA/HFMA-2	79.7 ± 2.0	65.4 ± 2.1	57.0 ± 2.1	42.1 ± 2.1	16.6 ± 0.3	16.1 ± 3.1	32.7 ± 1.2
BEMA/HFMA-3	80.3 ± 2.1	66.0 ± 2.0	61.6 ± 2.1	46.0 ± 2.1	13.7 ± 0.2	17.4 ± 3.1	31.1 ± 1.4
BEMA/HFMA-4	80.2 ± 2.0	66.2 ± 2.0	61.5 ± 2.1	46.2 ± 2.1	13.7 ± 0.2	17.4 ± 3.1	31.1 ± 1.3
BEMA/MAPS-1	78.2 ± 2.0	64.0 ± 2.1	63.0 ± 2.1	51.4 ± 2.0	9.0 ± 0.1	23.0 ± 3.4	32.0 ± 1.6
BEMA/MAPS-2	82.4 ± 2.0	70.4 ± 2.0	67.2 ± 2.1	56.3 ± 2.1	10.4 ± 0.1	18.1 ± 3.0	28.2 ± 1.5
BEMA/MAPS-3	85.3 ± 2.0	73.1 ± 2.0	70.5 ± 2.0	56.3 ± 2.1	11.1 ± 0.1	15.2 ± 2.8	26.2 ± 1.4
BEMA/MAPS-4	90.1 ± 2.1	76.2 ± 2.0	73.4 ± 2.1	61.5 ± 2.0	11.1 ± 0.1	12.5 ± 2.5	23.6 ± 1.3
BEMA/HFMA/MAPS-1	83.0 ± 2.1	71.4 ± 2.1	65.0 ± 2.1	54.5 ± 2.0	14.0 ± 0.2	14.4 ± 2.8	28.4 ± 1.3
BEMA/HFMA/MAPS-2	87.6 ± 2.1	75.0 ± 2.1	69.3 ± 2.0	57.2 ± 2.0	13.2 ± 0.2	12.4 ± 2.6	25.6 ± 1.2
BEMA/HFMA/MAPS-3	90.1 ± 2.0	78.0 ± 2.0	72.1 ± 2.0	60.6 ± 2.1	13.2 ± 0.1	10.6 ± 2.3	23.8 ± 1.2
BEMA/HFMA/MAPS-4	92.0 ± 2.0	78.1 ± 2.1	77.4 ± 2.0	63.5 ± 2.0	10.1 ± 0.1	12.0 ± 2.4	22.1 ± 1.3

containing segment, but also silicon-oxygen chain of MAPS towards the film surfaces [Fig. 4(c)]. Figure 5 displays total surface energies of the cured films. It is clearly seen that BEMA cured film has a much higher surface energy (44.1 mJ/m^2) than BEMA/HFMA, BEMA/MAPS and BEMA/HFMA/MAPS cured films do. According to Tavana's demonstration, when a liquid drop is applied to the surface, the outmost surface layer tends to interact with the liquid, and low-free energy of high hydrophobic surface gives a high contact angle with the liquid.[21] For the comparison between the sample BEMA/HFMA, BEMA/MAPS, and BEMA/HFMA/MAPS series, the surface energies of BEMA/HFMA and BEMA/MAPS cured films are in the range of 23.6–35.3 mJ/m^2, while BEMA/HFMA/MAPS cured films show lower surface energies down to 22.1 mJ/m^2 close to the surface energy of silicon (19.9 mJ/m^2),[22] indicating that the combination of HFMA and MAPS is beneficial for the further reduction of the surface energy of BEMA/HFMA/MAPS system.

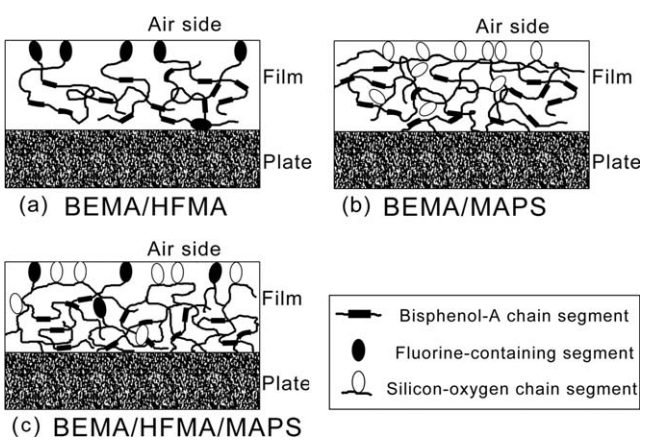

Figure 4 Schematic illustration of segments in the cured composite films.

Thermal behavior of UV-cured composite films

To study the thermal stability of the cured composite films, the TGA curves of neat BEMA, BEMA/HFMA-2, BEMA/MAPS-2 and BEMA/HFMA/MAPS system in the presence of gradual amount of MAPS are shown in Figure 6. The first stage of decomposition is from 100 to 160°C, attributing to the volatilization of the entrapped moisture present in the film. For the second stage above the temperature 360°C, the degradation belongs to the main part, in accordance with thermal cracking, dehydrogenation and gasification processes. The temperature values of the BEMA film at 5 wt % weight loss, 50 wt % weight loss, initial decomposition for the second step, maximum rate of weight loss for the second step and final decomposition for the second step are 218.2, 433.1, 380.5, 441.8, and 475.9°C, respectively. In the case of BEMA/HFMA cured films, the nature of single functionality of HFMA

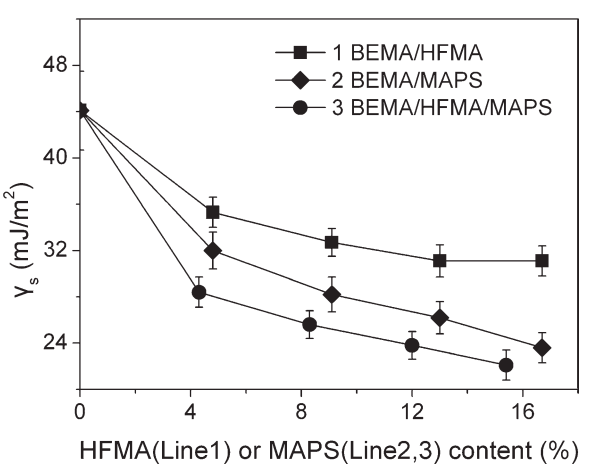

Figure 5 Relationship between the surface energy of the UV-cured composite films and the weight percentage of components.

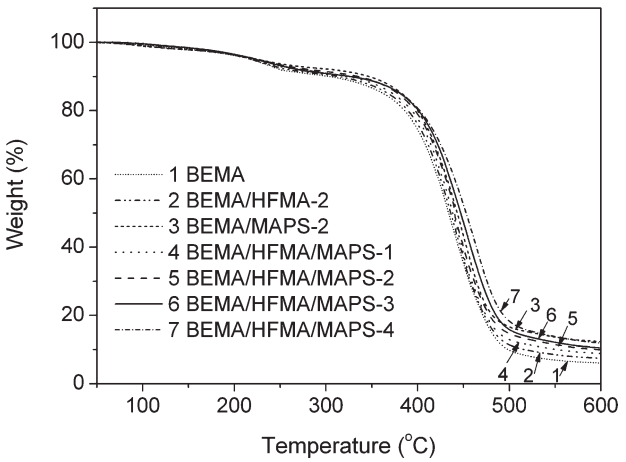

Figure 6 TGA curves of the UV-cured composite films.

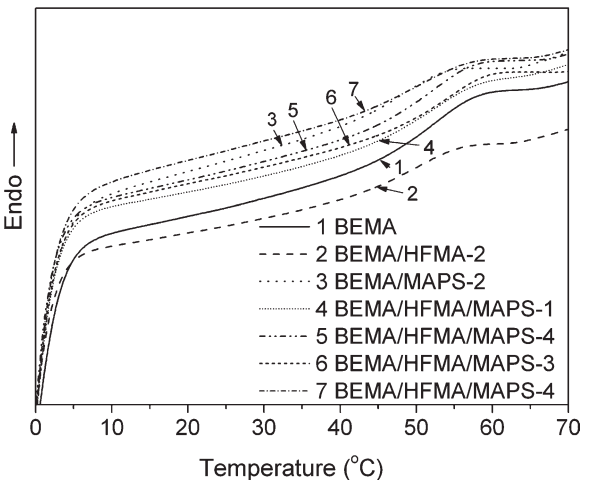

Figure 7 DSC curves of the UV-cured composite films.

did not significantly influence the thermal degradation of BEMA; like BEMA/HFMA-2 TGA curve, other proportion curves of BEMA/HFMA cured films are not shown. However, the thermal stabilities of BEMA/MAPS-2 and BEMA/HFMA/MAPS films were better than that of the neat BEMA film. Like the changes of BEMA/HFMA/MAPS TGA curves, other proportion curves of BEMA/MAPS cured films are not presented. In Figure 6, the BEMA/HFMA/MAPS decomposition curves show that additional 4.3–15.4 wt % of MAPS increased the temperatures of 5 and 50 wt % weight losses to 226.1 and 452.6°C, respectively, and the increased degree of initial decomposition, maximum rate of weight loss and final decomposition temperatures for the second step was between 13°C and 26°C. The good thermal stability in respect of BEMA/HFMA/MAPS cured films was possibly associated with the formation of stable three-dimensional network between BEMA and MAPS, since MAPS with the methacryloxy groups provided a great number of cross-link sites, corresponding to the report that quantitative cross-link agent used to epoxy resin UV-curing system could increase the thermal stability.[9]

In Figure 7, the value of T_g for BEMA/HFMA-2 cured film (47.6°C) is relatively lower than that of BEMA (48.5°C) (other curves of BEMA/HFMA are not shown due to the similarity). The T_g value (50°C) of BEMA/MAPS-2 is slightly higher than that of BEMA and similar to those of BEMA/HFMA/MAPS cured films (other curves of BEMA/BEMA are not shown due to the similarity), and with the increase of MAPS content the T_g values of BEMA/HFMA/MAPS basically stay within a narrow range of 50–52°C, which suggests that photocrosslinkable groups of MAPS can control the movement of BEMA chain, but its silicon-oxygen flexible chain enables T_gs of BEMA/MAPS and BEMA/HFMA/MAPS systems to rise slightly.

Water resistance property of UV-cured composite films

Table III lists the water resistance property of UV-cured composite films. After immersed in water for 5 days, except BEMA, BEMA/HFMA-1, and BEMA/MAPS-1 samples, all cured films had not any apparent change. It is noticeable that the immersed films did not break off from the selected substrates, implying that the presence of HFMA and MAPS still retained the hard adhesion function to substrates. In addition, the water absorption ratio of the cured films is one of the key parameter for characterization of the hydrophobicity. In Figure 8, the water absorption ratio curve of BEMA/HFMA cured films exhibits a slight change between 3.37 and 4.82%, while for BEMA/MAPS cured films the water absorption ratio has a great decrease from 2.76 to 1.36%. In terms of BEMA/HFMA/MAPS cured films, the influence of

TABLE III
Water Resistance Properties of The UV-Cured Composite Films

	Water resistance in 5 days		
	Substrates		
Sample	Glass	Copper	Wood
BEMA	Blanching	Blanching	Blanching
BEMA/HFMA-1	Blanching	Blanching	Blanching
BEMA/HFMA-2	Pass[a]	Pass	Pass
BEMA/HFMA-3	Pass	Pass	Pass
BEMA/HFMA-4	Pass	Pass	Pass
BEMA/MAPS-1	Blanching	Blanching	Blanching
BEMA/MAPS-2	Pass	Pass	Pass
BEMA/MAPS-3	Pass	Pass	Pass
BEMA/MAPS-4	Pass	Pass	Pass
BEMA/HFMA/MAPS-1	Pass	Pass	Pass
BEMA/HFMA/MAPS-2	Pass	Pass	Pass
BEMA/HFMA/MAPS-3	Pass	Pass	Pass
BEMA/HFMA/MAPS-4	Pass	Pass	Pass

[a] Pass: without blanching and breaking off.

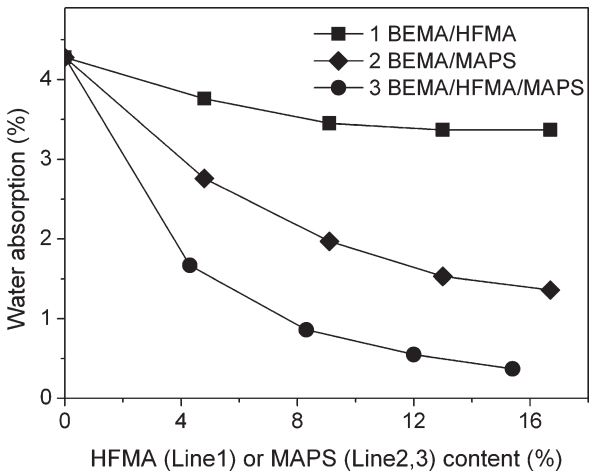

Figure 8 Relationship between the water absorption ratio of the UV-cured composite films and the weight percentage of components.

the absorption ratio by the content of MAPS was more significant. With increasing of MAPS content from 4.3 to 15.4 wt %, the water absorption ratios of corresponding samples decreased to 0.37%. As a result, both HFMA and MAPS can impart excellent water resistance to cured composite films, however high cross-link network caused by MAPS and BEMA plays a more important part in this point.

Micromorphology of UV-cured composite films

It was indicated that the macroperformances of blend films are closely relative to their micromorphology.[23] In our work, internal morphologies of the cured composite films were clearly demonstrated in SEM images. As shown in Figure 9(a), the cross section of neat BEMA film displays homogeneous morphology, while the dispersion of HFMA in BEMA is relatively uniform despite part of HFMA molecules towards the surface of the cured film [Fig. 9(b)]. It can be seen that the cross sections of BEMA/MAPS and BEMA/HFMA/MAPS cured films present unoriented and more compact than that of BEMA/HFMA cured film, which resulted from the good interaction between BEMA and MAPS because of their more chemical bonding sites [Fig. 9(c,d)]. This is in favor of good properties as our above discussions by contact angle, TGA, DSC, and water resistance analyzes. Additionally, we believe that the unoriented cross sections of BEMA/MAPS and BEMA/HFMA/MAPS cured films can facilitate the improvement of the flexibility for BEMA to some extent.

CONCLUSIONS

A series of BEMA/HFMA, BEMA/MAPS, and BEMA/HFMA/MAPS cured coating films were

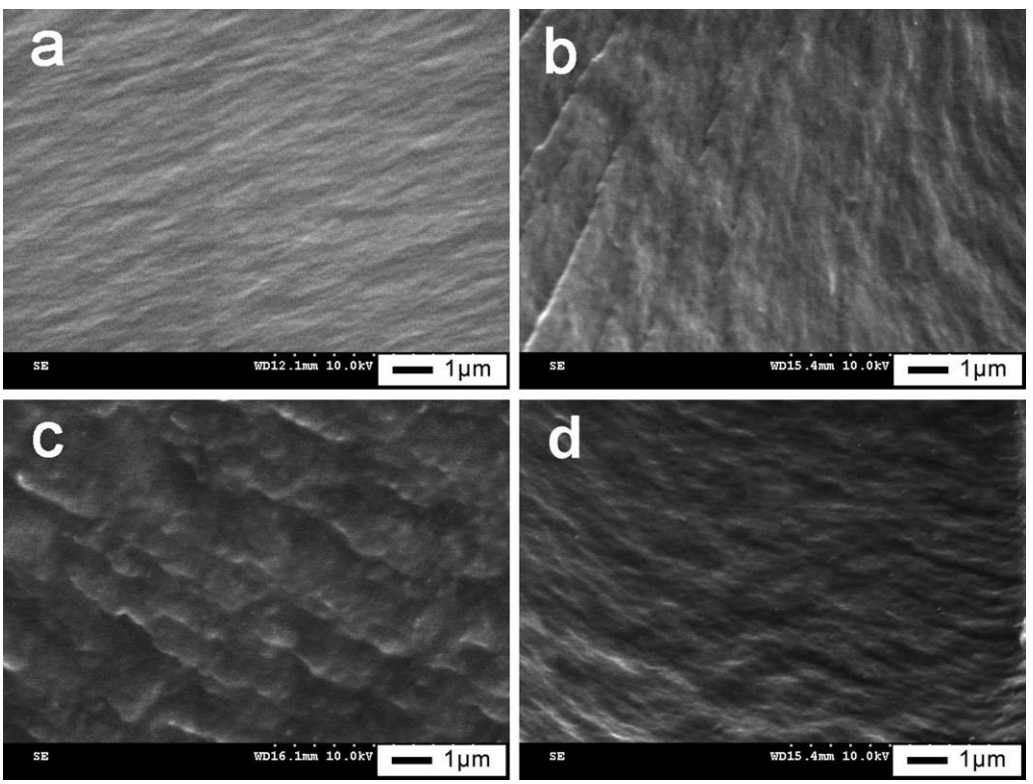

Figure 9 SEM images of cross section morphologies of the UV-cured composite films: (a) BEMA; (b)BEMA/HFMA-3; (c) BEMA/MAPS-3; (d) BEMA/HFMA/MAPS-3.

successfully fabricated via UV radiation. HFMA monomer was used to decrease surface energy of the UV-curing BEMA and enhance its water resistance property. Then the additive MAPS in BEMA matrix and BEMA/HFMA system could effectively modify the surface property and improve their thermal stabilities and water resistance properties due to the increased cross-link sites in the cured films. With respect to the observation of cross section morphology, HFMA dispersed in BEMA but lacking of cross-link sites; MAPS provided more cross-linkable groups leading to the good performances of BEMA/HFMA/MAPS cured coating materials. The research results are beneficial for developing great application of the UV-curable epoxy resin in areas such as coatings, adhesive, and packaging.

References

1. Ho, T. H.; Wang, C. S. J Appl Polym Sci 1994, 54, 13.
2. Levchik, S. V.; Weil, E. D. Polym Int 2004, 53, 1901.
3. Li, H. T.; Lin, M. S.; Chuang, H. R.; Wang, M. W. J Polym Res 2005, 12, 385.
4. Udagawa, A.; Sakurai, F.; Takahashi, T. J Appl Polym Sci 1991, 42, 1861.
5. Bajpai, M.; Shukla, V.; Kumar, A. Prog Org Coat 2002, 44, 271.
6. Lee, J. M.; Kim, D. S. Polym Compos 2007, 28, 325.
7. Kim, Y. H.; Kim, D. S. Polym Adv Technol 2008, 19, 1236.
8. Zou, J. H.; Zhao, Y. B.; Shi, W. F.; Shen, X. F.; Nie, K. M. Polym Adv Technol 2005, 16, 55.
9. Chattopadhyay, D. K.; Panda, S. S.; Raju, K. Prog Org Coat 2005, 54, 10.
10. Kayaman-Apohan, N.; Demirci, R.; Cakir, M.; Gungor, A. Radiat Phys Chem 2005, 73, 254.
11. Amerio, E.; Sangermano, M.; Colucci, G.; Malucelli, G.; Messori, M.; Taurino, R.; Fabbri, P. Macromol Mater Eng 2008, 293, 700.
12. Lu, D. P.; Xiong, P. T.; Chen, P. Z.; Huang, H. Z.; Shen, L.; Guan, R. J Appl Polym Sci 2009, 112, 181.
13. Kim, H. K.; Kim, J. G.; Cho, J. D.; Hong, J. W. Polym Test 2003, 22, 899.
14. Song, B. J.; Park, J. K.; Kim, H. K. J Polym Sci Polym Chem 2004, 42, 6375.
15. Bauer, F.; Mehnert, R. J Polym Res 2005, 12, 483.
16. Sun, F.; Jiang, S. L. Nucl Instrum Methods Phys Res B Beam Interact Mater At 2007, 254, 125.
17. Snyder, J. F.; Hutchison, J. C.; Ratner, M. A.; Shriver, D. F. Chem Mater 2003, 15, 4223.
18. Owens, D. K.; Wendt, R. C. J Appl Polym Sci 1969, 13, 1741.
19. Pinnau, I.; Freeman, B. D. (editor). In Proceedings of the 214th National Meeting of the American-Chemical-Society; Las Vegas, Nevada, 1997; p1.
20. Yokoyama, H.; Tanaka, K.; Takahara, A.; Kajiyama, T.; Sugiyama, K.; Hirao, A. Macromolecules 2004, 37, 939.
21. Tavana, H.; Simon, F.; Grundke, K.; Kwok, D. Y.; Hair, M. L.; Neumann, A. W. J Colloid Interface Sci 2005, 291, 497.
22. Wu, S. Interfacial Energy, Structure, and Adhesion Between Polymers; Academic Press: New York, 1978.
23. Zhou, Q.; Zhang, L.; Ming, Z. B.; Wang, B.; Wang, S. J. Polymer 2003, 44, 1733.